

SYSTEM CONSISTING OF SONIC SPARK CHAMBERS, TIME-OF-FLIGHT  
AND PULSE-HEIGHT COUNTERS ("MISSING-MASS SPECTROMETER")  
WITH ON-LINE COMPUTER

H. BLIEDEN, D. FREYTAG, F. ISELIN, F. LEFEBVRES,  
B. MAGLIC, H. SLETTENHAAR, S. ALMEIDA and A. LANG

CERN, Geneva

(presented by B. Maglič)

1. INTRODUCTION

We have built a system consisting of sonic spark chambers, time-of-flight, pulse-height and hodoscope counters (see Fig. 2). Such an instrument was proposed recently under the name of "missing-mass spectrometer"1), for the search of new unstable particles, X. (X can be boson, nucleon isobar or excited hyperon, depending on the type of the bombarding particle.)

We have in mind an investigation of the reaction



particle index:    1    2    3    4

with X = unstable boson.

In Fig. 2 we have listed the measurements which are supposed to be done by the MM-spectrometer. According to its function, the instrument can be divided into two parts:

- Part i) : "Pion line". It contains:  
- hodoscopes H<sub>1</sub> -H<sub>2</sub> -H<sub>3</sub> -H<sub>4</sub>  
- "vertex" counter, V.
- Part ii) : "Proton line". It contains:  
- sonic chambers S<sub>1</sub> -S<sub>2</sub> -S<sub>3</sub> -S<sub>4</sub>  
- hodoscopes for recoil proton R<sub>1</sub> -R<sub>2</sub> -R<sub>3</sub>  
- aluminium degraders D<sub>1</sub> -D<sub>2</sub> -D<sub>3</sub>, of variable thickness.

Part ii), the "Proton line", has been tested in a proton beam (with a 20% pion admixture) from the CERN Synchro-cyclotron. In Fig. 1, we show the diagram of this tested part of the system.

## 2. QUANTITIES INVOLVED IN THE MEASUREMENT OF MISSING-MASS

Mass of particle 4,  $M_4$ , in Reaction (1) is equal to the missing-mass of particle 3,  $m_3$ . In general,  $(\text{miss. mass})^2 = (\text{miss. energy})^2 - (\text{miss. momentum})^2$ , which, for the case of Reaction (1), ( $M_2 = M_3$ ) becomes:

$$m_3^2 = M_4^2 = M_1^2 - 2 \left[ \left( P_1^2 + M_1^2 \right)^{\frac{1}{2}} + M_1 \right] \left[ \left( P_3^2 + M_3^2 \right)^{\frac{1}{2}} - M_3 \right] + 2P_1 P_3 \cos \Theta_3. \quad (2)$$

All quantities in Eq. (2) are in the laboratory system. Knowledge of  $m_3$  requires simultaneous measurement of six quantities; they are listed in Table 1, together with the description of the measuring technique used.

All measured quantities listed in Table 1 are first digitized and then registered in scalars. The existing CERN scalar readout logic is used to transfer the information from the scalars, either onto magnetic tape or to the Mercury computer.

In the following text we describe only the essential facts about the operation of our system. Overall description of the interconnections and parts of the instrument will not be given. Apart from the descriptive figures 1 and 2, the reader is referred to talks presented by F. Iselin in Session IV and by H. Slettenhaar in Session V.

## 3. DATA STORAGE

All raw data without any pre-selection or pre-computation, are stored from the scalars onto the magnetic tape. We use the IBM unit, placed in an air-conditioned trailer. The tape speed is 36"/sec with a density of 200 characters per inch. A 2,400 ft reel can store  $3 \times 10^4$  events (from 30 scalars).

Assuming a 100% running efficiency and 100 msec for the recording of an event, one expects, on the average, 2 events per 300 msec/burst of the Proton-Synchrotron, or 3,600 events/hour. Our estimate is a 30% efficiency; thus, the expected data getting rate is 1,000 events/hour or 2.4  $\times 10^4$  events/day.

#### 4. ROLE OF THE ON-LINE COMPUTER

Due to the slowness of the Ferranti "Mercury" computer used, only one out of three to four events can be processed to the point of computing  $M_3$ , Eq. (1). This makes the computer a sampling facility. The importance of sampling is two-fold:

- i) It makes it possible to test the goodness of the physics result (missing-mass distributions) by applying certain prescribed checks on the  $\Theta_3$  vs  $P_3$  dot density distributions. The proposed method of "particle hunting" depends on these tests (described in paragraph 5). The  $\Theta$  vs  $P$  display is done by the mechanical x-y plotter.
- ii) It constantly checks the functioning of the whole instrument: whenever an event cannot be "fitted", the reason for the failure (type of error) is displayed (see paragraph 6) on the typewriter on-line.

#### 5. ON-LINE CHECKS AGAINST FALSE PEAKS

We know, today, only of two  $X^-$  resonances ( $I = 1$ ):  $\rho$  and  $B$ , whose masses are 750 and 1,220 MeV, respectively, and width  $\Gamma = 100$  MeV. If there are no new resonances, the Number vs  $m_3$  distribution would show a continuum (phase space), with only these two peaks superimposed on it. A new heavy boson would show as another peak on the continuum.

However, in the past bubble-chamber work, peaks in  $N$  vs  $MM$  distribution frequently turned out to be false ones. (All unstable bosons were found in the effective mass, rather than  $MM$  distributions.)

The proposed method prescribes definite tests, to be made in the course of the experiment, which should be capable of revealing if the peak is false or not.

#### $\Theta_3$ vs $P_3$ scatter diagram

In this technique, the result is not displayed in the usual  $N$  vs  $MM$  histogram. Since, at fixed  $P_1$ ,  $MM$  is a function of only two variables,  $MM = f(\Theta_3, P_3)$ , each event can be represented by a dot in a  $\Theta_3$ - $P_3$  plane. This gives more information than  $N$  vs  $MM$  histogram. First, it shows, simultaneously, cross-section as a function of the momentum transfer  $\Delta^2$  ( $\sim P_3^2$ ). Secondly, the scatter diagram provides two independent tests:

Test 1: If there is a discreet mass in X, the dots should lie along one mass-line whose shape is well known at any incident  $P_1 = \text{fixed}$ . (See, for example,  $\Theta_3$ - $P_3$  mass lines for  $P_1 = 6 \text{ GeV}$  in Fig. 3.) An increase of dot-density, if the effect is real, is expected along a given line. If this condition appears to be satisfied in the course of the run, the physicist proceeds to

Test 2: The mass-lines shift in a known manner with the change of the incident momentum  $P_1$ ; the increase (decrease) of  $P_1$  by  $1 \text{ GeV/c}$ , typically increases (decreases) the maximum angle by about  $3^\circ$ . At any beam setting, the variation of the beam momentum of  $\pm 1 \text{ GeV/c}$  is possible without changes in the beam design.

Therefore, the second test consists of repeating the run at  $P_1 + 1 \text{ GeV/c}$  and  $P_1 - 1 \text{ GeV/c}$ , and seeing if the density distribution follows the scale prescribed by kinematics. For example, the dotted line in Fig. 3 shows the shift of the  $1.5 \text{ GeV}$  mass line for  $P_1 = 8 \text{ GeV/c}$ , in respect to the one at  $P_1 = 6 \text{ GeV/c}$  (solid line), i.e. it shows the effect of  $\Delta P = + 2 \text{ GeV/c}$ .

## 6. OPERATION OF THE "PROTON LINE"

Here, we shall describe the procedure of identifying the proton and computing its  $\Theta_3$  and  $P_3$  in its time sequence:

From the sonic information obtained from 24 transducers in chambers  $S_1$ ,  $S_2$ ,  $S_3$  and  $S_4$ , the spark co-ordinates (x,y) in each of the six gaps are fitted; then a straight line (proton direction) is fitted through the points;

- The straight line is extrapolated into the  $R_1$  hodoscope; the programme computes which of the three counters should have been hit by the particle; on the other hand, the programme checks the information stored in the pattern unit and sees if the observed counter number,  $R_{1i}^{\text{obs}}$  is equal to  $R_{1i}^{\text{expected}}$ . If yes, the position of the particle in the plane of the  $R_{1i}$  counter is computed; then, the time of propagation of the light signal from this point to the photo-multiplier is subtracted from the observed time-of-flight,  $(\text{TOF})^{\text{obs}}$ . This gives "first-corrected TOF".
- The straight line is then extrapolated forward to the target to find the intersection with the incident pion direction. [This is the vertex of Reaction (1)]; then the time-of-flight taken for the pion to travel from  $H_4$  to the vertex is subtracted from the first corrected TOF. This gives the real time-of-flight,  $(\text{TOF})^{\text{real}}$ .

- Check is made on the counter number  $R_{2i}$  which is hit by the proton.
- Using the  $(TOF)^{real}$  and the information on the thickness of degrader  $D_2$ , the expected pulse height,  $(PH)_2^{exp}$ , in hodoscope  $R_2$  is computed, on the assumption that the particle is proton; then, the information on the  $(PH)_2^{observed}$  is compared, and if they agree to 20%, proton is identified.
- Similar procedure is repeated for the hodoscope  $R_3$ ; then,
- $P_3$  is computed.
- $\Theta_3$  is computed.

#### 7. USE OF TYPEWRITER ON-LINE

The typewriter is in the experimental area, on-line with the computer output; it gives the evidence on the functioning of every instrument of the system at any time:

- i) whenever an event cannot be "fitted" by the missing-mass programme, the reason for the failure is typed. This can be illustrated by the following examples:
  - If the pion line operates properly only one counter in each of the hodoscopes  $H_1$  -  $H_4$  should go off. If, in one hodoscope, (say  $H_3$ ), two counters, (say 2 and 4), give signals, the event will not be fitted.  
  
Error H324 will be typed.
  - There were two sparks in  $S_2$ . This will give too short sonic times.  
  
Error type: 6S2
  - One transducer, say No. 1 in  $S_3$ , has become insensitive or disconnected. This gives too long sonic time.  
  
Error type: 5S31
  - One spark chamber gap became inefficient. This would result in the absence of the stop signals in any of the four microphones in that gap.  
  
Error type: 5.

- An event does not satisfy the PH criterion for proton of given TOF.

Error type: 9.

- ii) The repetition of any of these errors draws the experimentalist's attention to the specific part of the apparatus. He requests the computer operator to output the quantities related to the part of the system which is malfunctioning. He can plot the distribution of each of the quantities.

An example of this is given in Figs. 4 and 5. Distribution has revealed that the spark chamber  $S_1$  was inclined by  $1^\circ$  to the vertical.

#### ACKNOWLEDGEMENTS

Thanks are due to G.R. Macleod for suggesting and helping to organize the use of the Mercury computer; to D. Harting for his help in the planning of the system; to B. Levrat\*) for his help in the later stages; J. Tischhauser for his constructions; J.W. Beck, L. Dubal\*), F. Marciano and G. Genova for their invaluable assistance.

Reference 1) : CERN Memorandum MM-1 (1963).

---

\*) University of Geneva.

Table 1

Physical quantities involved in measuring "missing-mass spectrum"

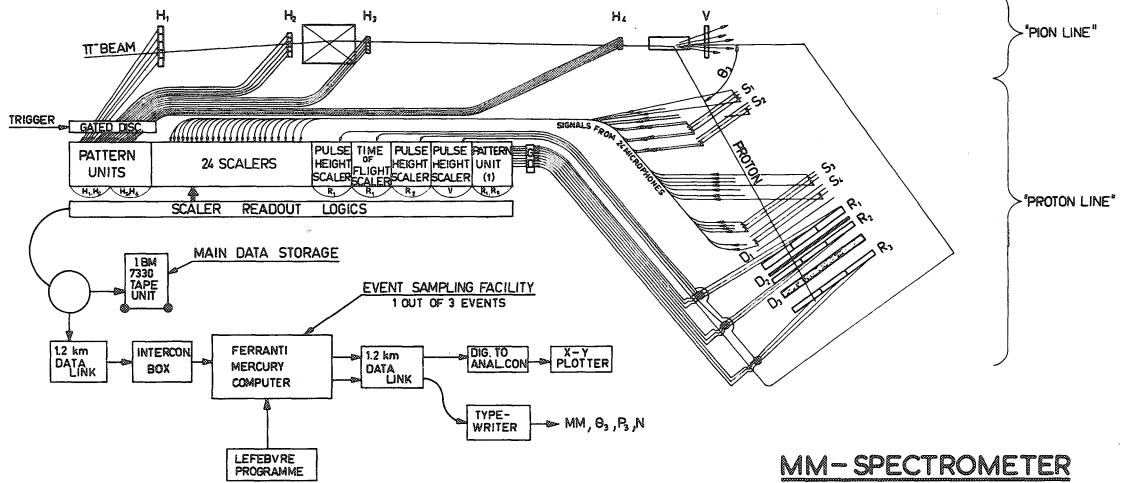
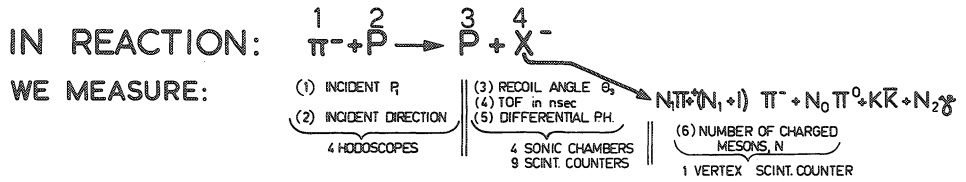
Observable	Method of measuring	Accuracy
1. Mass of incident pion, $M_1$	Not measured. Beam is presumed to contain 99.3% pions.	
2. Momentum of incident pion, $P_1$	Magnet 120 mrad, with 4 counter hodoscopes $H_1, H_2, H_3, H_4$	$\pm 1\%$
3. Direction of incident pion, $\hat{P}_1$	2 counter hodoscopes $H_3 - H_4$	$\pm 1$ mrad
4. Mass of recoil proton, $M_3$	Differential pulse-height (3 hodoscopes $R_1 - R_2 - R_3$ ) and time-of-flight	$\pm 20\%$
5. Momentum of recoil proton, $P_3$	Time-of-flight	$\pm 0.5$ nsec
6. Direction of recoil proton, $\hat{P}_3$ (measurements 3 and 6 give angle $\Theta_3$ )	2 three-gap sonic spark chambers	$\pm 1$ mrad
7. Number of charged particles, $N$ , into which X-boson decays (not directly related to the measurement of $m_3$ ) but essential to our method of eliminating background.	Pulse-height counter	In 5% cases one more particle will be counted due to Landau tail.

Figure captions

- Fig. 1 Simplified version of missing-mass spectrometer, tested 19-20 December, 1963. Results of the test are given in Figs. 4-11. See also Fig. 2.
- Fig. 2 Complete diagram of the data reduction system for MM-spectrometer. The "proton line" was tested (see Fig. 1).
- Fig. 3 Kinematic "mass-lines" in the  $\Theta_3$  vs  $p_3$  plane at incident pion momentum of  $p_1 = 6$  GeV/c. An example for the shift of the mass-line is shown for  $p_1 = 8$  GeV/c (dotted line). See paragraph 4 of the text.
- Fig. 4 } Distribution of the differences of the spark positions in two  
Fig. 5 } gaps in the sonic chamber of active area of  $40 \times 80$  cm<sup>2</sup>, for the x and y coordinates, respectively. The systematic shift of 1 mm in the y coordinate helped us in finding out that the chamber was inclined 1° to the vertical.
- Fig. 6 Distribution of the differences of the shock-wave parameter  $\Delta t$  in two gaps.  $\Delta t$  is proportional to the square root of the spark energy (see Lillethun et al., Operation of a sonic spark-chamber system, CERN report 1963).
- Fig. 7 Angular distribution of the collimated proton beam, as measured by two sonic spark-chamber gaps, 150 cm apart. This measurement gives our angular resolution to be  $\pm 0.05^\circ$ .
- Fig. 8 Pulse-height distribution in a scintillator  $50 \times 30$  cm<sup>2</sup>, 1 cm thick, obtained with protons of 0.9 GeV/c. This gives our pulse-height distribution, which is  $\pm 23\%$ .
- Fig. 9 Momentum resolution, obtained by time-of-flight measurements.
- Fig. 10 Flow diagram of the MM-programme used in the test of "proton line". The set-up is shown in Fig. 1.
- Fig. 11 Missing-mass resolution, obtained with the proton line set-up, described in Fig. 1.
- Fig. 12 Layout of the cable connecting four experimental areas on the CERN site to Mercury computer (M). Details of the link are described by Slettenhaar, Session V.



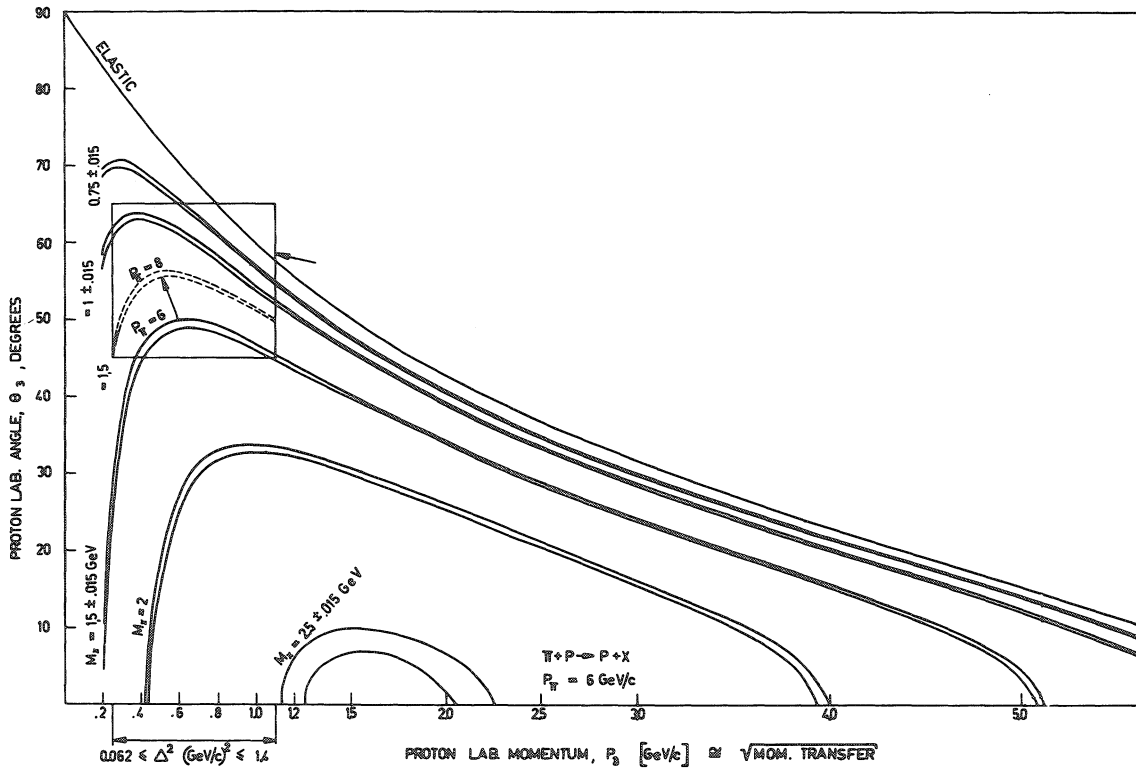




[ TRIGGER LOGICS (A-OUTPUTS) ARE NOT SHOWN ]

**MM-SPECTROMETER**  
GENERAL DIAGRAM OF B-OUTPUTS (DATA REDUCTION)

Fig. 2



Experiment uses "kinetic splitting" of the mass lines: angular resolution needed for  $\Delta M = \pm 15 \text{ MeV}$  is  $\pm 0.5^\circ$ ; momentum resolution needed for the same mass resolution is typically 20% to 45%.

Dotted line is the line corresponding to mass of 1.5 GeV at incident momentum of 8 GeV/c. All solid lines correspond to incident momentum of 6 GeV/c. The mass line shifts  $\sim 3^\circ$  per 1 GeV/c. This property provides a check of the effect in MM-distribution, if some observed.

Fig. 3

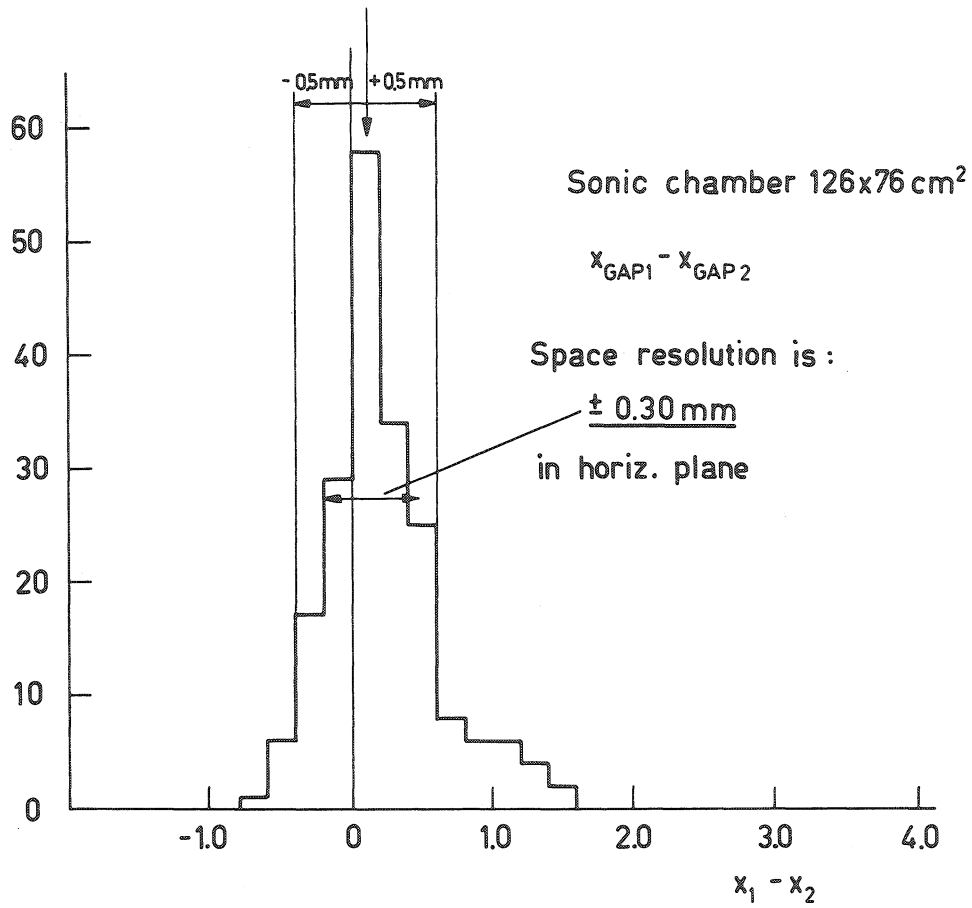


Fig. 4

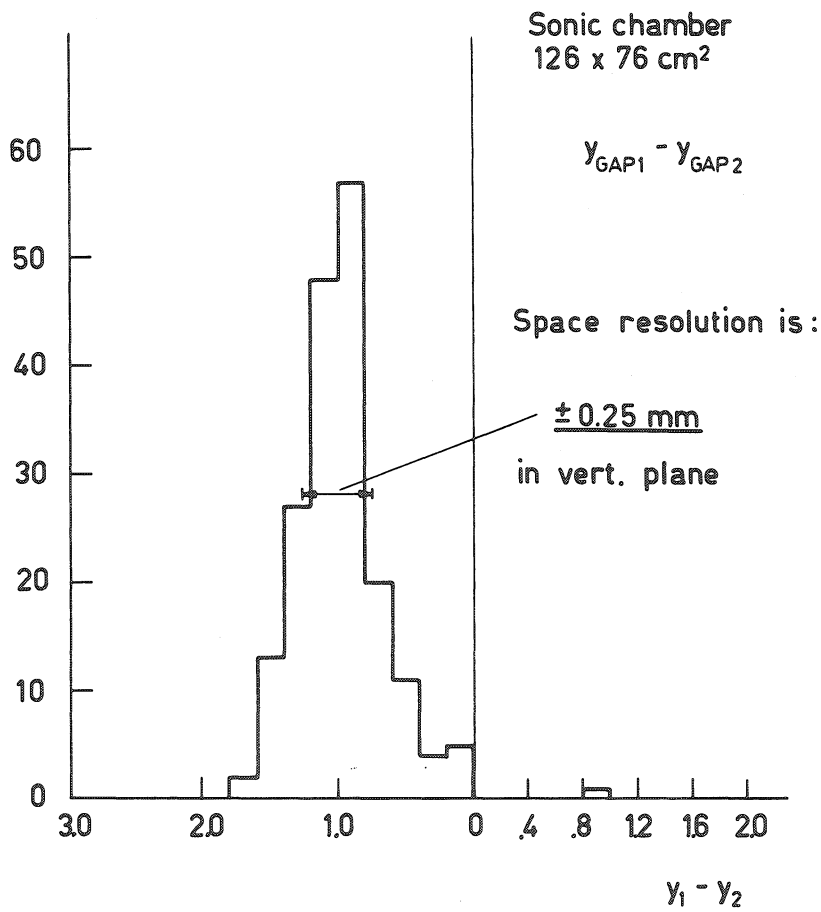


Fig. 5

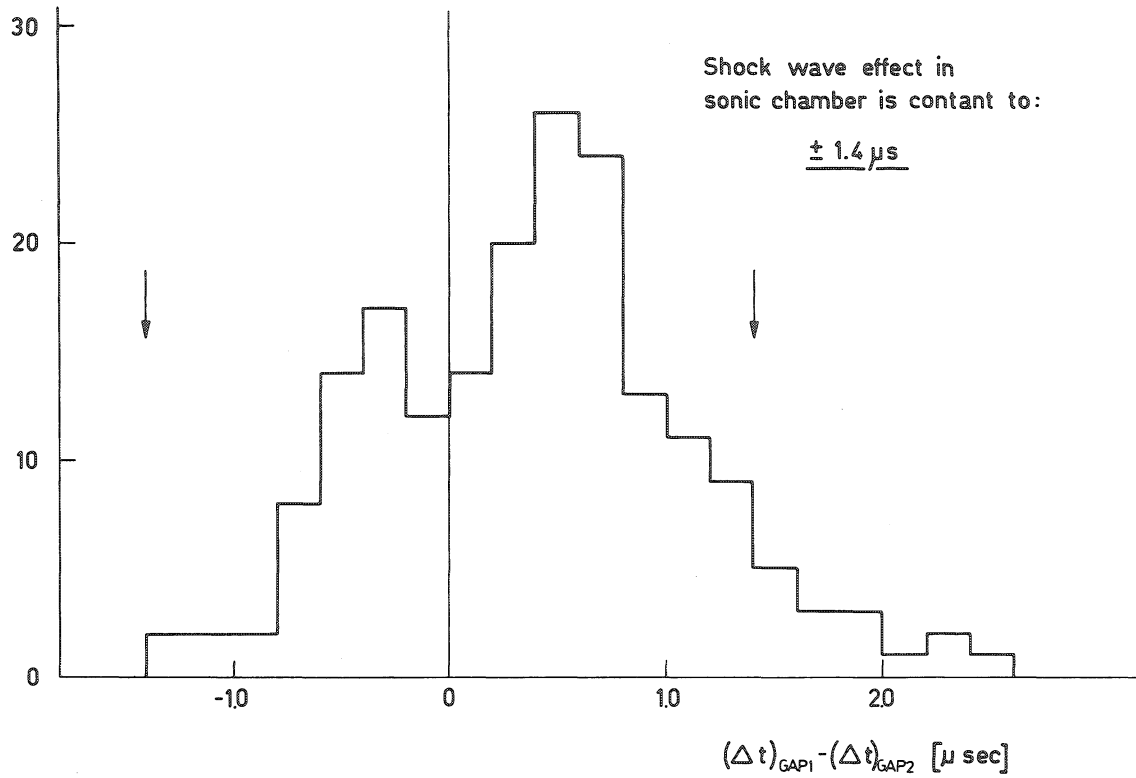


Fig. 6

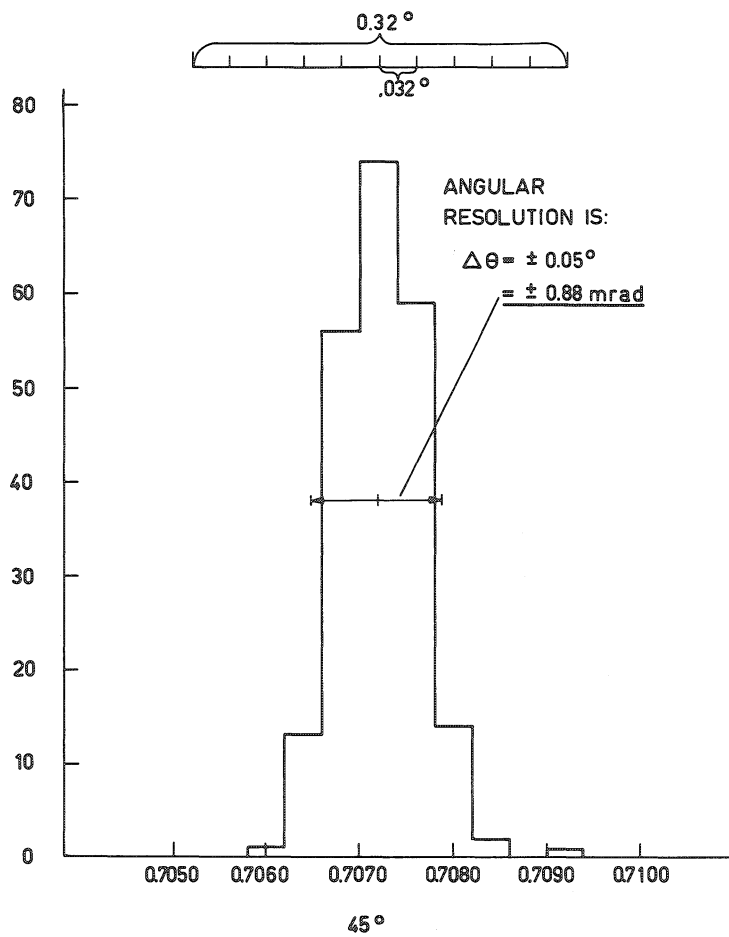


Fig. 7

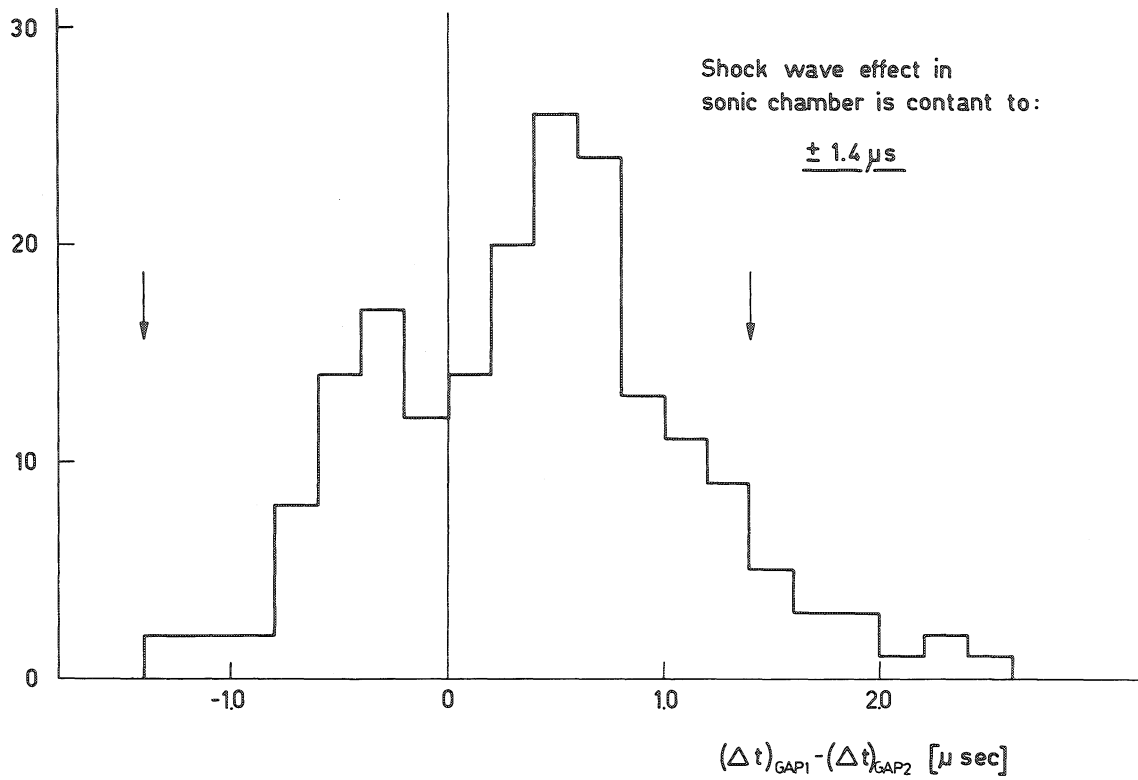


Fig. 6

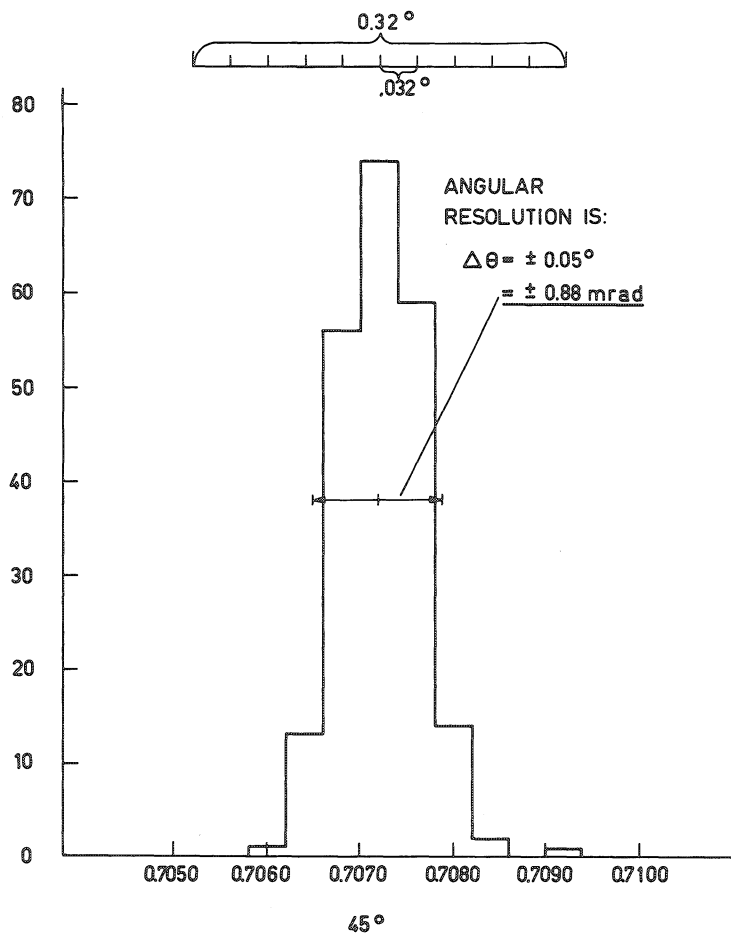


Fig. 7

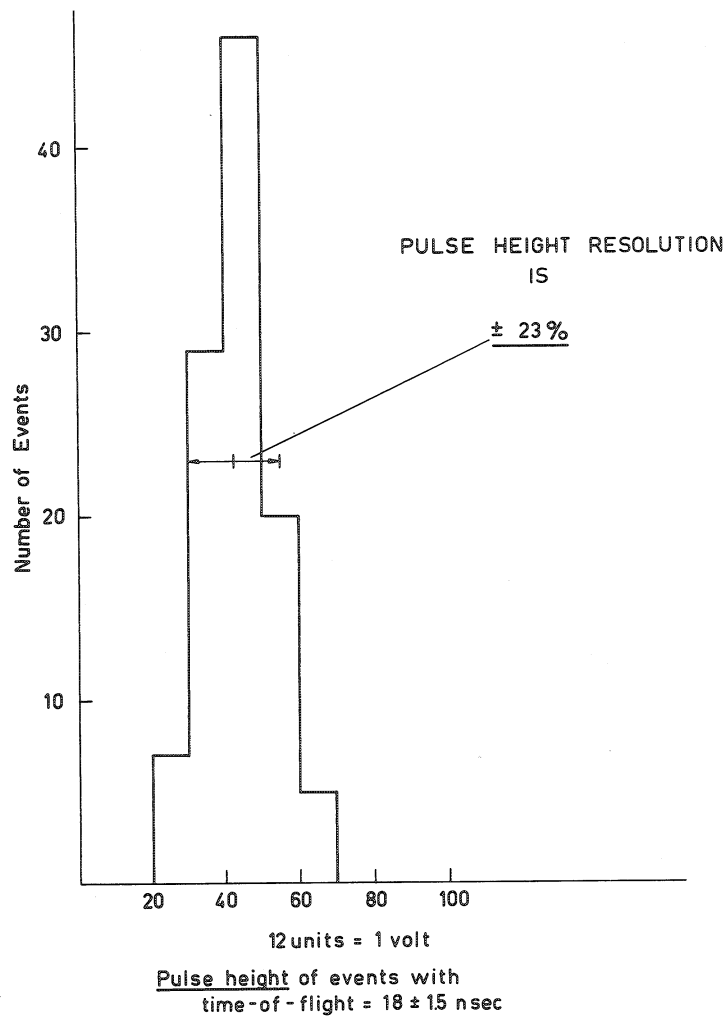


Fig. 8

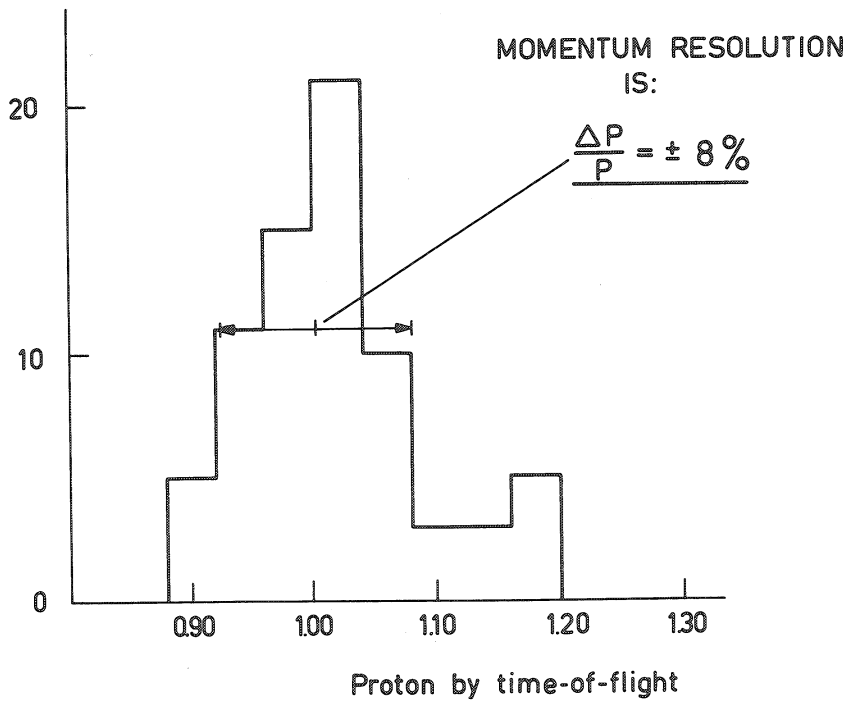


Fig. 9

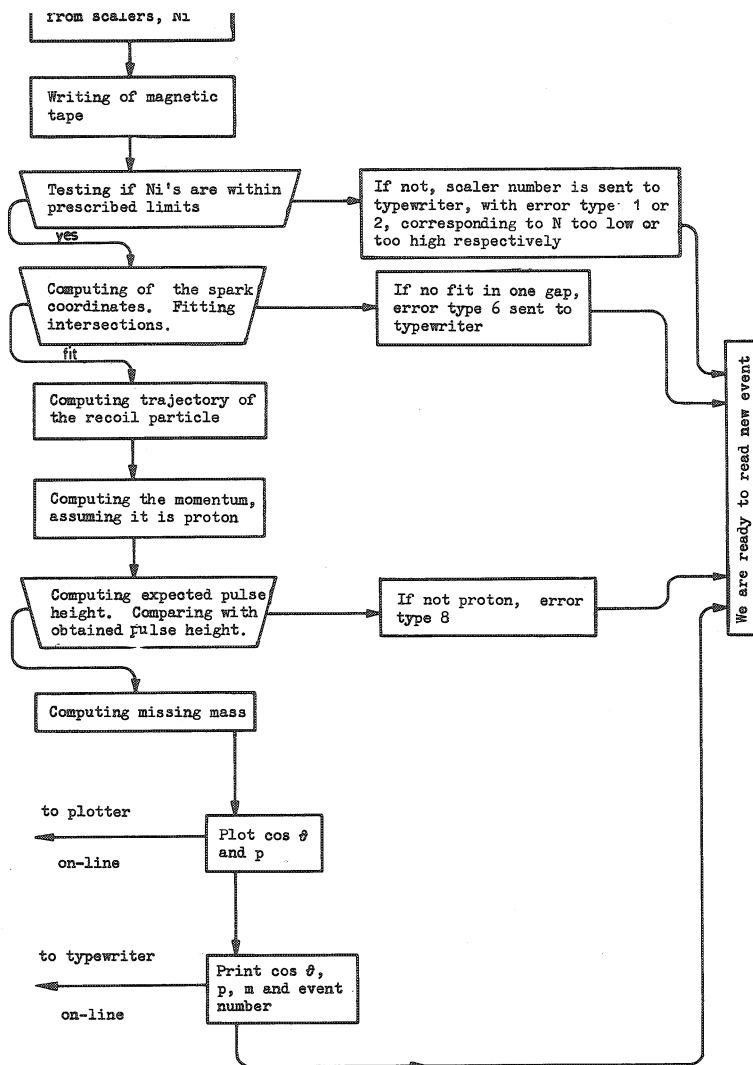


Fig. 10

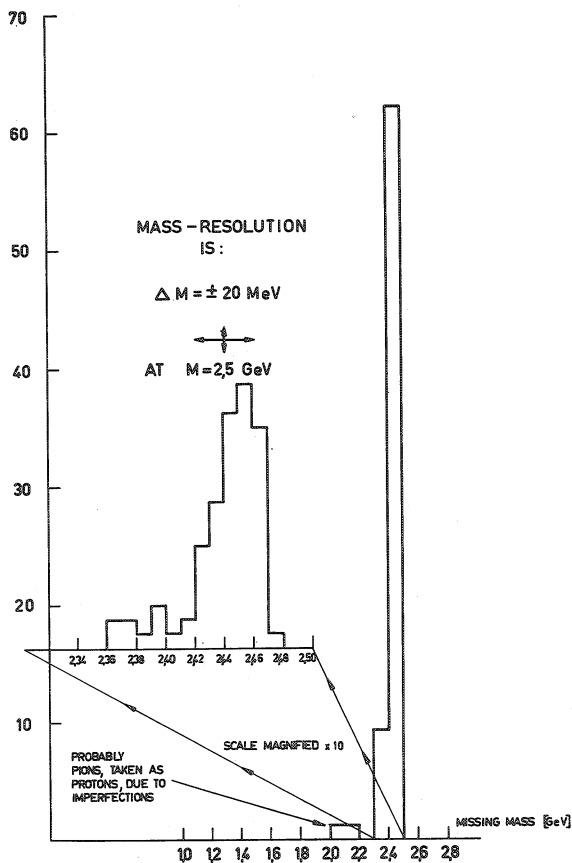


Fig. 11

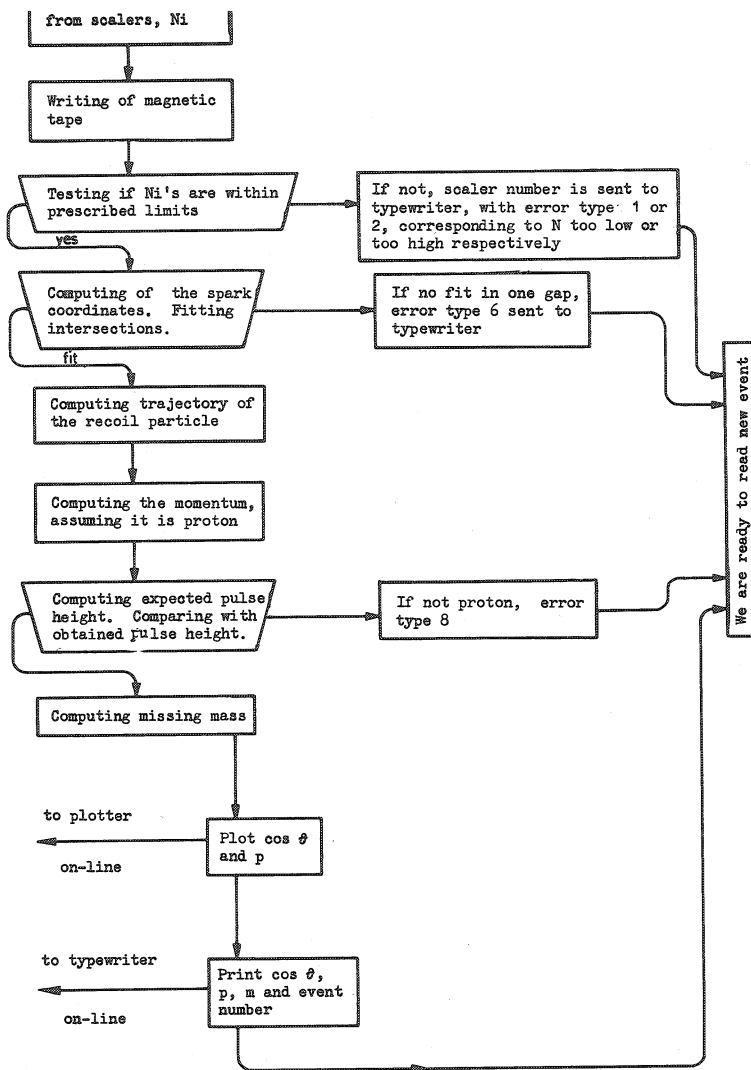


Fig. 10

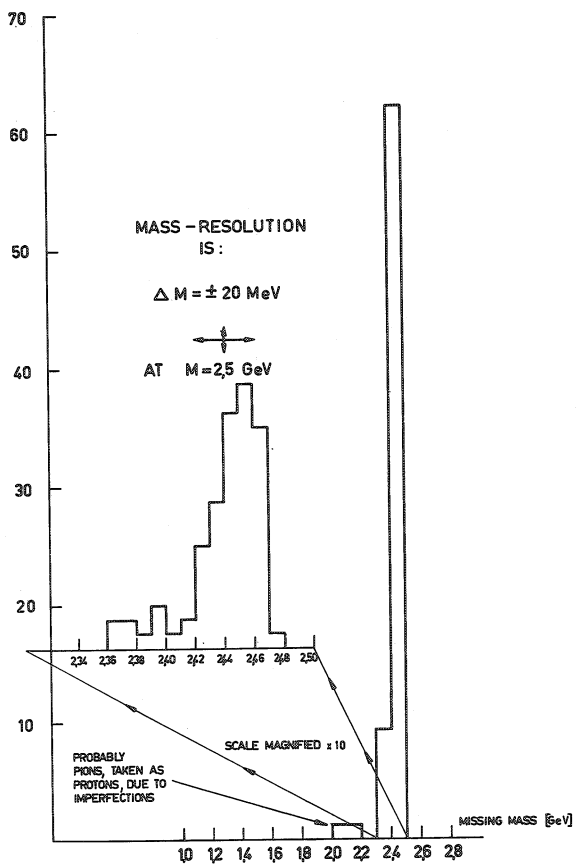


Fig. 11



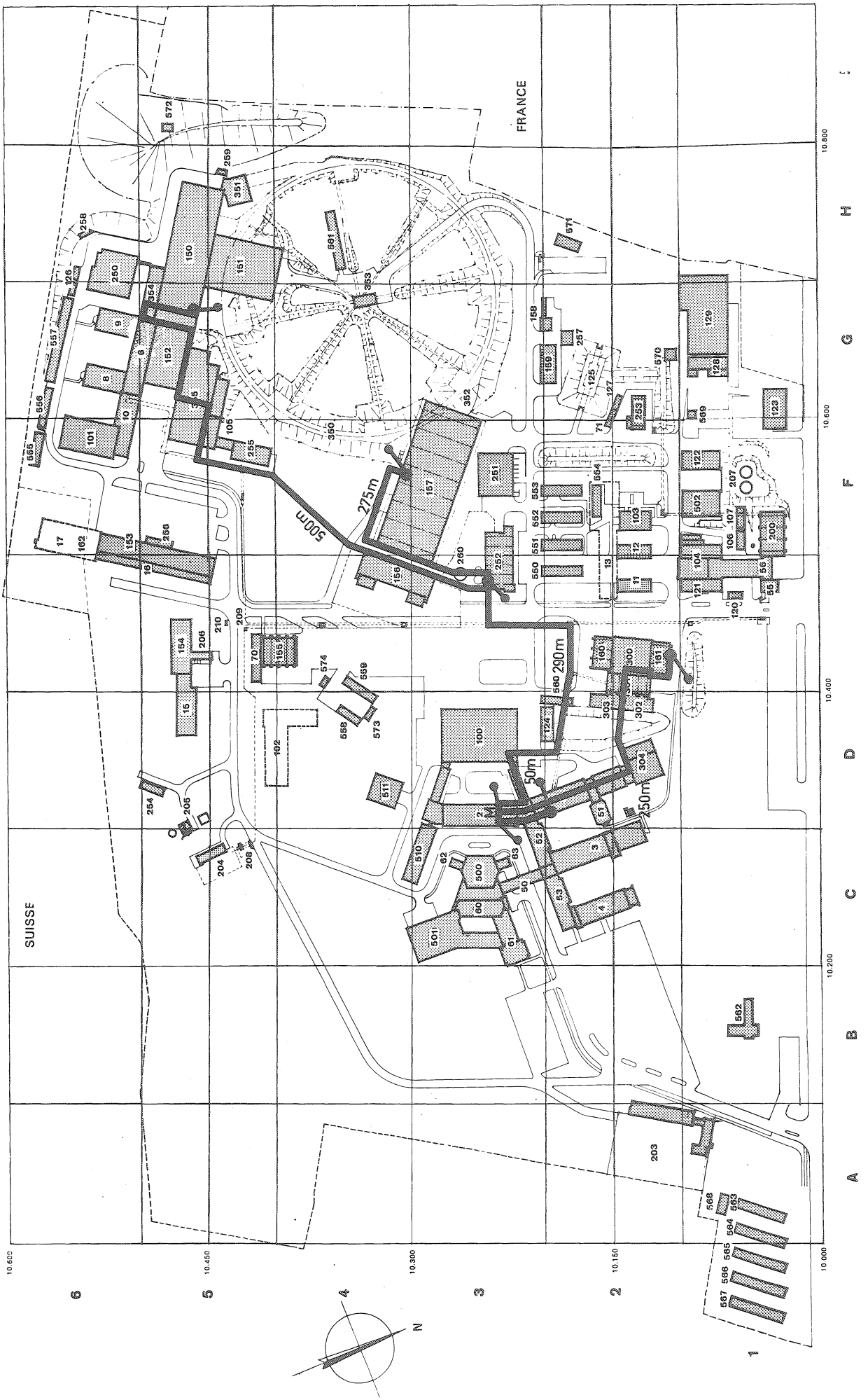


FIG. 12

GENÈVE